Turk J Phys
32 (2008) , 341 – 356.
© TÜBİTAK

Dielectric Dispersion in PbO-Bi_2O_3-B_2O_3 Glasses Mixed with TiO_2

P. Venkateswara RAO, M. Srinivasa REDDY, V. Ravi KUMAR, Y. GANDHI, N. VEERAIAH
Department of Physics, Acharya Nagarjuna University–Nuzvid Campus, Nuzvid-521 201, A.P, INDIA
e-mail: nvr8@rediffmail.com

Received 27.02.2008

Abstract

$[(PbO)_{0.20-x}\cdot(Bi_2O_3)_{0.40}\cdot(B_2O_3)_{0.40}]$:$(TiO_2)_x$, $0.0 \leq x \leq 0.02$ glasses were prepared. Dielectric properties (dielectric constant $\varepsilon\prime$, loss tan δ and a.c. conductivity σ_{ac}, over a wide range of frequency and temperature), optical absorption, ESR and IR spectra of these glass materials have been investigated. The dielectric study has revealed that the glasses possess high insulating strength when TiO_2 concentration is >0.8 mol% in the glass matrix. The optical absorption spectra of these glasses exhibited bands due to Ti^{3+} ions in the visible region. ESR spectral studies have also indicated that a fraction of Ti^{4+} ions reduced to Ti^{3+} ions. IR spectra of these glasses exhibited bands due to TiO_4 and TiO_6 structural units. Quantitative studies indicate that as concentration of TiO_2 is increased to 0.8 mol% in the glass matrix, a large proportion of titanium ions exist in Ti^{3+} state and has influenced the physical properties of these glasses to a substantial extent.

1. Introduction

Bi_2O_3–B_2O_3 glasses exhibit transmission into the far infrared region (0.5–8.7 μm), possess high refractive index and exhibit nonlinear optical behavior. Recently, optical Kerr shutter switching and degenerated four-wave mixing experiments have been performed on bismuth borate glasses using femtosecond pulse lasers [1–3]. In view of these characteristics, Bi_2O_3 based glasses have potential applications in optoelectronic circuits as ultrafast switches, infrared windows, optical isolators [2, 3]. The nonconventional glass forming oxide Bi_2O_3, participates in the glass structure with two possible coordinations $[BiO_3]$ pyramidal and $[BiO_6]$ octahedral units [2–4]. Further, bismuth ion was found to be an efficient luminescent activator with applications in lasers as a sensitizer for some rare earth ions [5, 6]. Kityk et al have carried out extensive work on Bi_2O_3 based glasses along these lines [7] in recent years.

Titanium oxide (1 mol% or more), in general, is considered a nucleating agent of crystallization in silicate glass materials [8]. However, the presence of small quantities of TiO_2 in other glass matrices, such as borophosphates, is observed to enhance glass forming ability and chemical durability of the glasses [9]. Normally, ions of titanium exist in the glass networks in Ti^{4+} state and participate in glass network forming with TiO_4, TiO_6 and sometimes with TiO_5 (comprising of trigonal bipyramids) structural units [10, 11]. However, there are reports suggesting that these ions may also exist in Ti^{3+} state in some glass matrices [12, 13]. The presence of Ti^{4+} ions makes glass to be suitable for non-linear optical devices, since the empty

or unfilled d-shells of these ions contribute more strongly to nonlinear polarizabilities. Usually, the d-orbital contribution to non-linear polarizability is found to be more for bond lengths less than 2 Å [14]; the bond length of Ti-O is estimated to be 1.96 Å. Literature survey on the glasses containing TiO_2 indicates that these glasses possess negative non-linear refractive index that induces self-focusing radiation beam in the material; as a result, the devices can be operated at a smaller input power [15, 16]. Nevertheless, the investigation on the co-ordinate chemistry of Ti^{4+} and Ti^{3+} ions in Bi_2O_3–B_2O_3 glass network is of interest in itself because, these ions are expected to influence the physical properties of the glasses to a large extent. A detailed literature survey indicates that no devoted studies are available on the influence of titanium ions on the dielectric properties of bismuth borate glasses.

The study of dielectric properties, such as constant, loss and a.c. conductivity over a wide range of frequency and temperature not only help in assessing the insulating character of the glasses but also throw some light on the structural aspects of these glasses [17–21]. The current investigation is aimed at an understanding the influence of the titanium ions on structural aspects of PbO–Bi_2O_3–B_2O_3 glasses by studying their dielectric and spectroscopic properties.

2. Experimental Methods

Within the glass forming region of PbO–Bi_2O_3–B_2O_3 glass system, the following compositions with successive increase in the concentration of TiO_2 are chosen for the present study:

T_0: $[(PbO)_{0.20-x}\cdot(Bi_2O_3)_{0.40}\cdot(B_2O_3)_{0.40}]:(TiO_2)_0$

T_2: $[(PbO)_{0.198}\cdot(Bi_2O_3)_{0.40}\cdot(B_2O_3)_{0.40}]:(TiO_2)_{0.002}$

T_4: $[(PbO)_{0.196}\cdot(Bi_2O_3)_{0.40}\cdot(B_2O_3)_{0.40}]:(TiO_2)_{0.004}$

T_6: $[(PbO)_{0.194}\cdot(Bi_2O_3)_{0.40}\cdot(B_2O_3)_{0.40}]:(TiO_2)_{0.006}$

T_8: $[(PbO)_{0.192}\cdot(Bi_2O_3)_{0.40}\cdot(B_2O_3)_{0.40}]:(TiO_2)_{0.008}$

T_{10}: $[(PbO)_{0.190}\cdot(Bi_2O_3)_{0.40}\cdot(B_2O_3)_{0.40}]:(TiO_2)_{0.010}$

T_{12}: $[(PbO)_{0.188}\cdot(Bi_2O_3)_{0.40}\cdot(B_2O_3)_{0.40}]:(TiO_2)_{0.012}$

T_{15}: $[(PbO)_{0.185}\cdot(Bi_2O_3)_{0.40}\cdot(B_2O_3)_{0.40}]:(TiO_2)_{0.015}$

T_{20}: $[(PbO)_{0.180}\cdot(Bi_2O_3)_{0.40}\cdot(B_2O_3)_{0.40}]:(TiO_2)_{0.02}$

Appropriate amounts (all in mol%) of reagent grades of PbO, Bi_2O_3, H_3BO_3 and TiO_2 powders were thoroughly mixed in an agate mortar and melted in a platinum crucible in the temperature range 950–1000 °C in a PID temperature controlled furnace for about 1 h until a bubble free transparent liquid was formed. The resultant melt was then poured in a brass mould and subsequently annealed at 300 °C (i.e. below its glass transition temperature). The amorphous state of the glasses was confirmed by X-ray diffraction and scanning electron microscopy studies (see Figures 1 and 2).

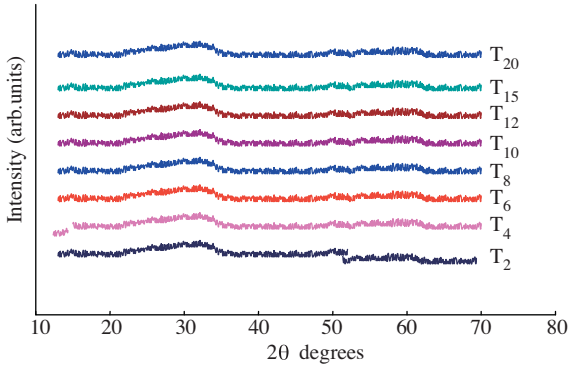

Figure 1. X-ray diffraction patterns of $[(PbO)_{0.20-x}\cdot(Bi_2O_3)_{0.40}\cdot(B_2O_3)_{0.40}]:(TiO_2)_x$ glasses.

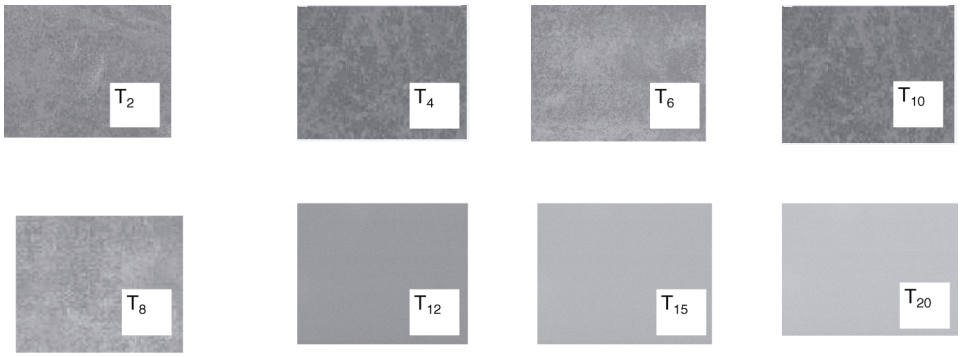

Figure 2. SEM photographs of $[(PbO)_{0.20-x}\cdot(Bi_2O_3)_{0.40}\cdot(B_2O_3)_{0.40}]$:$(TiO_2)_x$ glasses.

The samples were then ground and optically polished. The final dimensions of the samples used for dielectric and optical studies were about 1 cm × 1 cm × 0.2 cm. The density d of the glasses was determined to an accuracy of 0.001 by standard principle of Archimedes' using o-xylene (99.99% pure) as the buoyant liquid. Infrared transmission spectra for these glasses were recorded using a Perkin-Elmer 1600 Infrared Spectrophotometer in the wavenumber range 400–4000 cm^{-1} by KBr pellet method. The ESR spectra of the fine powders of the samples were recorded at room temperature on a JEOL JM-FX3 X-band ($\nu = 9.234$ GHz) ESR spectrometer with 100 kHz field modulation. A thin coating of silver paint was applied (to the larger area faces) on either side of the glasses to serve as electrodes for dielectric measurements. The painted samples were then dried with a hot blower for about 10 minutes on either side. The details of dielectric measurements were given in our earlier reports [22, 23]. Measurement accuracy of the dielectric constant is ∼0.001 and that in loss is $\sim 10^{-4}$. The optical absorption spectra of the glasses were recorded at room temperature in the wavelength range 350–1200 nm up to a resolution of 0.1 nm using a Shimadzu model 3101 UV-vis-NIR Spectrophotometer.

3. Results

Based on the glass density d and calculated average molecular weight $\bar{M}$, various physical parameters, such as titanium ion concentration N_i and mean titanium ion separation r_i, are evaluated for understanding the physical properties of these glasses using the conventional formulae and the values obtained are presented in Table 1.

Table 1. Various physical parameters of PbO-Bi_2O_3-B_2O_3 glasses mixed with TiO_2.

Sample	Avg. Mol. Wt	Density (g/cm^3)	Conc. of Ti ions (Ni, $10^{21}/cm^3$)	Inter ionic distance Ti ions $r_{i(A^\circ)}$	Polaron radius r_p
T_2	258.6	6.439	2.99	6.94	2.80
T_4	258.3	6.428	5.99	5.51	2.22
T_6	258.0	6.417	8.98	4.81	1.94
T_8	257.7	6.407	11.97	4.37	1.76
T_{10}	257.4	6.396	14.95	4.06	1.64
T_{12}	257.2	6.385	17.93	3.82	1.54
T_{15}	256.7	6.369	22.40	3.55	1.43
T_{20}	256.0	6.342	29.83	3.22	1.30

The dielectric constant $\varepsilon\prime$ and loss tan δ at room temperature (≈30 °C) of $(PbO)_{0.20}\cdot(Bi_2O_3)_{0.40}\cdot(B_2O_3)_{0.40}$ (i.e., TiO_2 free) glass at 100 kHz are measured to be 7.46 and 0.006, respectively; the values of these parameters are found to increase considerably with decrease in frequency. The values of $\varepsilon\prime$ and tan δ are observed

to increase with the concentration of TiO_2 gradually up to 0.8 mol%; and for further increase of TiO_2, these two parameters have been observed to decrease.

Temperature dependence of $\varepsilon\prime$ of the glasses containing different concentrations of TiO_2 at 10 kHz is shown in Figure 3. The value of $\varepsilon\prime$ is found to exhibit a considerable increase at higher temperatures; the rate with which $\varepsilon\prime$ increases with temperature is found to be the highest for the glass containing 0.8 mol% of TiO_2.

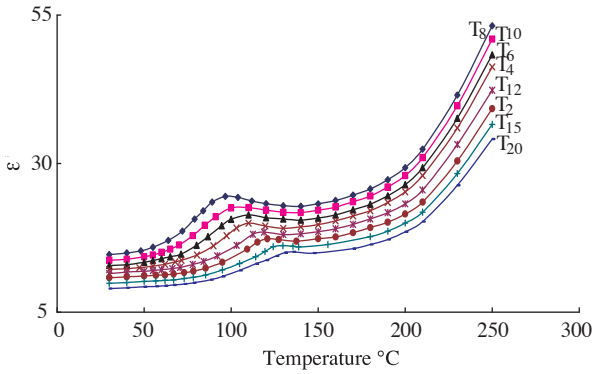

Figure 3. A comparison plot of variation of dielectric constant (at 10 kHz) with the temperature for $[(PbO)_{0.20-x}\cdot(Bi_2O_3)_{0.40}\cdot(B_2O_3)_{0.40}]$:$(TiO_2)_x$ glasses. Inset gives the variation of dielectric constant with temperature at different frequencies of glass F_8.

Temperature dependence of tan δ of all the glasses measured at a frequency of 1 kHz is shown in Figure 4. The dielectric loss curves of TiO_2-containing glasses exhibited distinct maxima. With increasing frequency the temperature maximum shifts towards higher temperature, and with increasing temperature the frequency maximum shifts towards higher frequency, indicating the dielectric relaxation character of dielectric losses of these glasses. Additionally, the observations on dielectric loss variation with temperature indicated an increase in the broadness and $(\tan\delta)_{\max}$ of relaxation curves with increase in the concentration of TiO_2 up to 0.8 mol%. Using the relation

$$f = f_{\bigcirc}\exp(-W_d/KT), \tag{1}$$

the effective activation energy W_d for the dipoles is calculated for different concentrations of TiO_2; the activation energy is found to increase with increase in the concentration of TiO_2 beyond 0.8 mol% (inset of Figure 3 and Table 2).

Table 2. Data on dielectric loss of PbO-Bi_2O_3-B_2O_3: TiO_2 glasses.

Glass	$(\text{Tan}\,\delta)_{\max}$	A.E. for dipoles (eV)	A.E. for Conduction (eV)	Spreading factor b
T_2	0.013	2.72	0.324	0.52
T_4	0.018	2.45	0.268	0.62
T_6	0.021	2.26	0.246	0.68
T_8	0.025	1.98	0.218	0.72
T_{10}	0.026	2.13	0.236	0.69
T_{12}	0.023	2.53	0.286	0.58
T_{15}	0.012	2.86	0.334	0.51
T_{20}	0.010	2.98	0.352	0.49

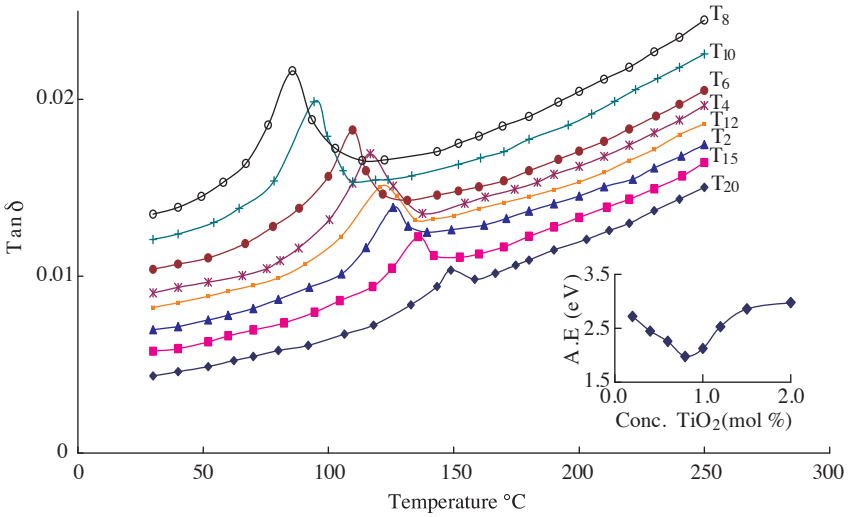

Figure 4. A comparison plot of variation of dielectric loss (at 1 kHz) with the temperature for $[(PbO)_{0.20-x}\cdot(Bi_2O_3)_{0.40}\cdot(B_2O_3)_{0.40}]:(TiO_2)_x$ glasses. Inset shows the variation of activation energy for dipoles with the concentration of TiO_2.

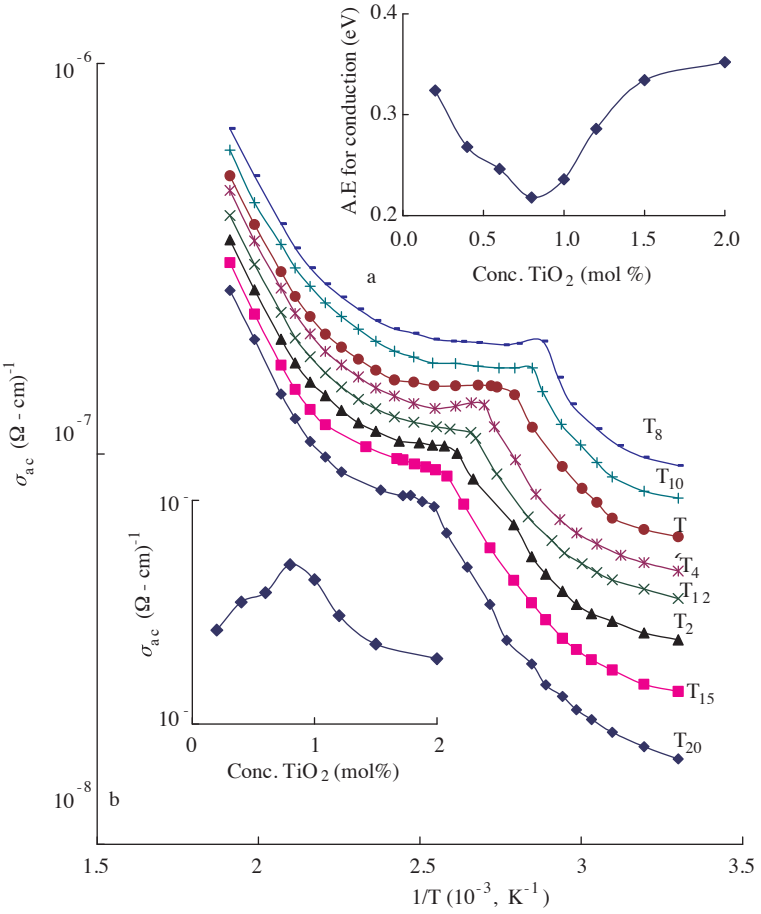

Figure 5. Variation of σac with $1/T$ at 10 kHz for $[(PbO)_{0.20-x}\cdot(Bi_2O_3)_{0.40}\cdot(B_2O_3)_{0.40}]:(TiO_2)_x$ glasses. Inset (a) shows the variation of activation energy for conduction, (b) shows the variation of s ac with the concentration of TiO_2.

The a.c. conductivity σ_{ac} is calculated at different temperatures using the equation

$$\sigma_{ac} = \omega \varepsilon\prime \varepsilon_o \tan \delta \tag{2}$$

A plot of log σ_{ac} against $1/T$ for all the glasses at 10 kHz is shown in Figure 5. The conductivity is found to increase considerably at any given frequency and temperature with increase in the concentration of TiO_2 from 0.2 to 0.8 mol%. From these plots the activation energy for conduction in high temperature region over which a near linear dependence of log σ_{ac} with $1/T$ could be observed is evaluated and its variation with the concentration of TiO_2 is shown as the inset 'a' of Figure 5; the curve exhibits a minimum at 0.8 mol% of TiO_2.

The optical absorption spectra of $[(PbO)_{0.20-x}\cdot(Bi_2O_3)_{0.40}\cdot(B_2O_3)_{0.40}]:(TiO_2)_x$ glasses recorded at room temperature in the wavelength range 400–900 nm are shown in Figure 6. The spectrum of TiO_2 free glasses has not exhibited any absorption bands. However, due to the TiO_2 mixing, the spectrum of each glass exhibited two clearly resolved absorption bands at about 530 and 690 nm. These bands are assigned to transitions $^2B_{2g} \rightarrow {}^2B_{1g}$ and $^2B_2g \rightarrow {}^2A_{1g}$ of Ti^{3+} ions [24–26]. With a gradual increase in the concentration of TiO_2 in the range 0 to 0.8 mol%, the half width and intensity of these two bands are observed to increase. Pertinent data related to optical absorption spectra of these glasses are furnished in Table 3.

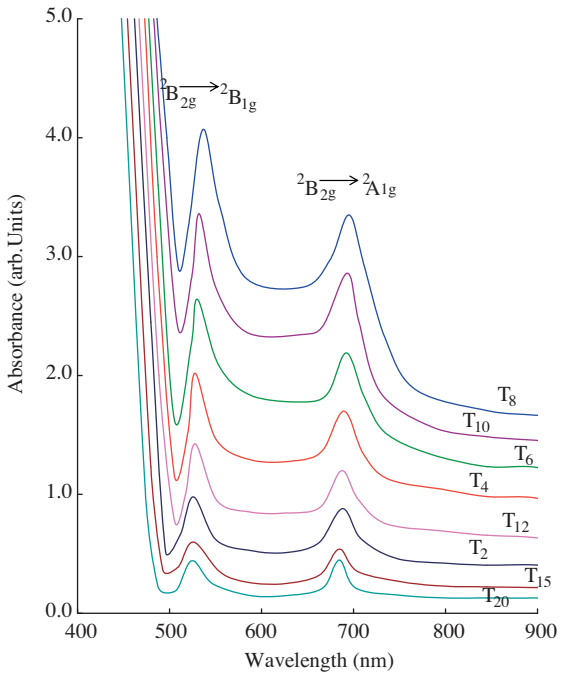

Figure 6. Optical absorption spectra of $[(PbO)_{0.20-x}\cdot(Bi_2O_3)_{0.40}\cdot(B_2O_3)_{0.40}]:(TiO_2)_x$ glasses.

From the observed absorption edges in optical absorption spectra, we have evaluated the optical band gaps E_o of these samples by drawing Urbach plots (Figure 7) between $(\alpha\hbar\omega^{1/2}$ and $\hbar\omega$ is per the equation

$$\alpha(\omega)\,\hbar\omega = c\,(\hbar\omega - E_o)^2\,. \tag{3}$$

From the extrapolation of the linear portion of the curves of Figure 7, the values of optical band gap E_o are determined and are presented in Table 3. The value of the E_o is observed to be the minimum for glass T_8.

Table 3. Summary of the data on optical absorption spectra of TiO_2 mixed PbO-Bi_2O_3-B_2O_3 glasses.

Glass	Cut-off wavelength (nm)	Optical band gap E_o (eV)	Position of $^2B_{2g} \rightarrow {}^2B_{1g}$ band (nm)	Position of $^2B_{2g} \rightarrow {}^2A_{1g}$ band (nm)
T_2	461	2.37	526	686
T_4	473	2.28	527	689
T_6	477	2.26	530	692
T_8	486	2.22	537	695
T_{10}	482	2.23	532	693
T_{12}	466	2.31	526	687
T_{15}	454	2.42	525	684
T_{20}	447	2.45	524	682

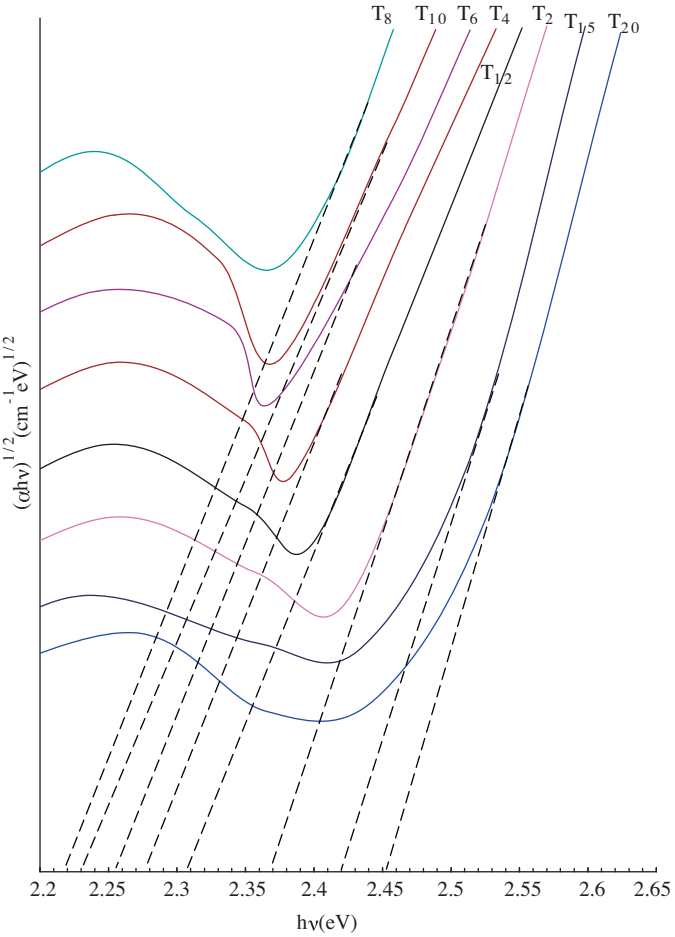

Figure 7. Urbach plot of $[(PbO)_{0.20-x}\cdot(Bi_2O_3)_{0.40}\cdot(B_2O_3)_{0.40}]:(TiO_2)_x$ glasses.

The ESR spectra (Figure 8) of $[(PbO)_{0.20-x}\cdot(Bi_2O_3)_{0.40}\cdot(B_2O_3)_{0.40}]:(TiO_2)_x$ glasses recorded at room temperature exhibited a signal consisting of a central line at about $g_\perp = 1.942$. The intensity and the half width $\Delta B_{1/2}$ of the central line are observed to increase considerably with the increase in the concentration of TiO_2 up to 0.8 mol%, and beyond this concentration the intensity of the signal is observed to be feeble.

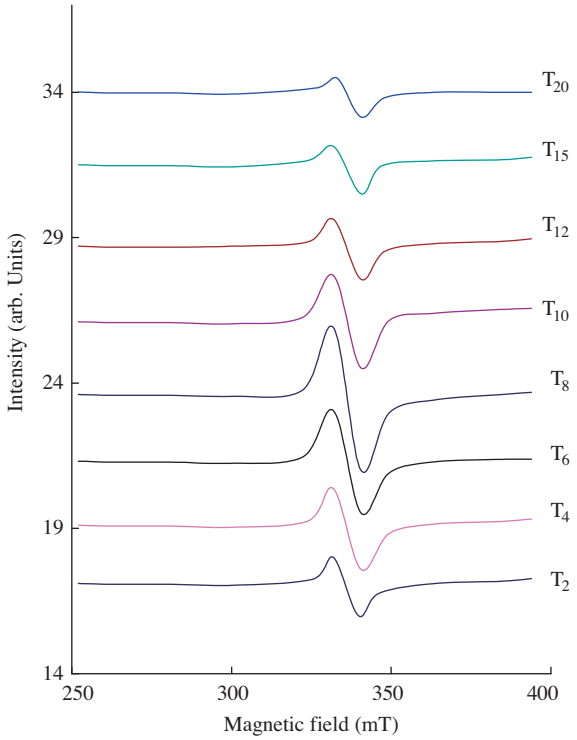

Figure 8. ESR spectra of $[(PbO)_{0.20-x}\cdot(Bi_2O_3)_{0.40}\cdot(B_2O_3)_{0.40}]$:$(TiO_2)_x$ glasses.

Infrared transmission spectra of pure $(PbO)_{0.20}\cdot(Bi_2O_3)_{0.40}\cdot(B_2O_3)_{0.40}$ (viz., TiO_2 free) glass, seen in Figure 9, exhibited three bands: (i) in the region 1300–1400 cm^{-1}, due to the conventional stretching relaxation of B-O bond of the trigonal BO_3 units, (ii) in the region 1000–1100 cm^{-1}, due to the vibrations of BO_4 structural units and (iii) a band at about 710 cm^{-1} arising from the bending vibrations of B-O-B linkages [27, 28].

A band due to PbO_4 structural units is also observed in the spectra of all the glasses at about 470 cm^{-1} [29, 30]; in this minor region, a band due to symmetrical bending vibrations of BiO_6 units was also reported [31]. In view of this we may also expect the presence of Bi-O-Pb linkages in the glass network.

In general, TiO_4 units exhibit four normal vibrational bands at about 750 cm^{-1} ($\nu_s(A_1)$), 306 cm^{-1} ($\delta_d(A)$), 770 cm^{-1} ($\nu_d^{as}(F)$) and at 370 cm^{-1} ($\delta_d(F)$) [32]; all of which are active in the Raman spectrum, but only $\nu_d^{as}(F)$ and $\delta_d(F)$ were found to be active in the IR spectrum. On the other hand, TiO_6 units are anticipated to exhibit six normal vibrational bands, but only $\nu_d^{as}(F)$ and $\delta_d(F)$ modes were reported to be active in the IR spectrum. In the IR spectrum of the glass T_2, two additional prominent bands were observed at 739 and 638 cm^{-1}. Further, it was also established that, in the IR spectra of glasses and their crystalline products, the bands due to TiO_6 units lie around 650 cm^{-1}, whereas the bands due to TiO_4 units lie in the high frequency region [33–35]. Based up on the literature survey, the first band at 739 cm^{-1} is identified due to Ti-O-Ti symmetric stretching vibrations within TiO_4 units, whereas the later band is attributed to the vibrations of Ti-O bonds in deformed octahedra [36–38].

With increase in the concentration of TiO_2 up to 0.8 mol%, the intensity of the band due to TiO_4 structural units is observed to decrease and that of TiO_6 structural units is observed to increase. However, a reversal trend in the intensity of these two bands has been observed, with further rise in the concentration of TiO_2. It may be worth mentioning here that the band due to TiO_4 structural units is observed to shift towards lower wavenumber (for sample T_{20}) where the vibrational band due to B-O-B is also present; as a result, we may attribute the band at about 720 cm^{-1} (especially in the spectra of glass T_{20}) to the common vibrations of B-O-Ti units (see Figure 9).

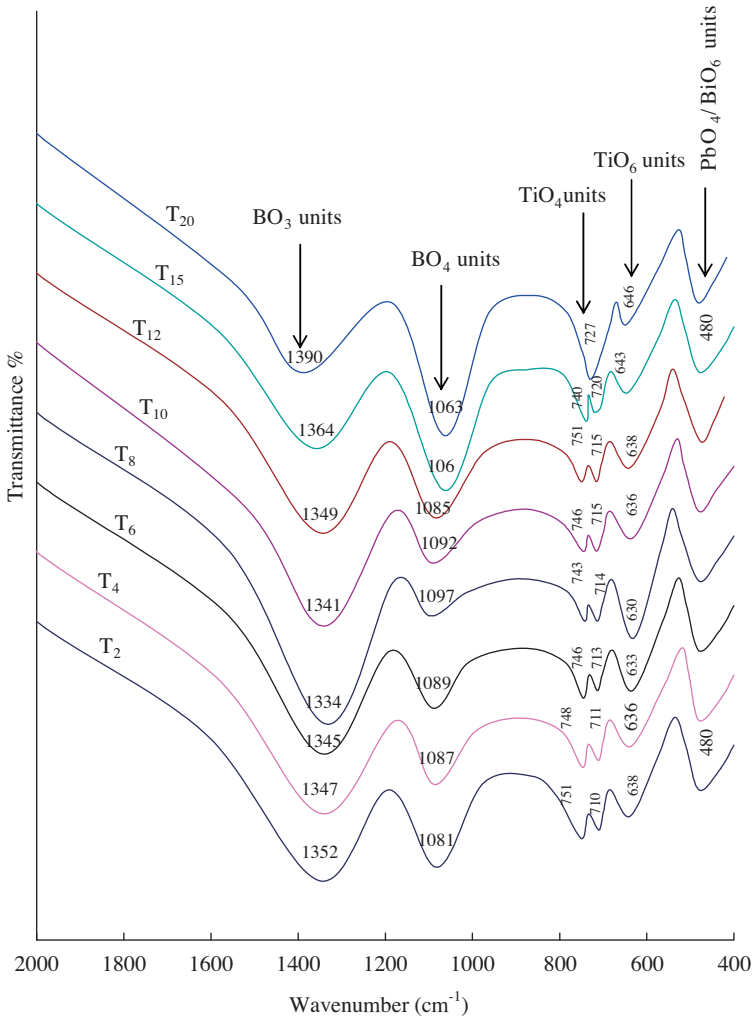

Figure 9. IR spectra of $[(PbO)_{0.20-x}\cdot(Bi_2O_3)_{0.40}\cdot(B_2O_3)_{0.40}]$:$(TiO_2)_x$ glasses.

4. Discussion

As per the studies reported by Bray et al [39], the fraction of the four fold coordinated boron in PbO-B_2O_3 is ∼0.53. Accordingly, the structural–chemical composition of this glass can be represented in the form of a combination of the following structural chemical units:

$$0.5Pb^{+2}_{1/2}[BO_{4/2}]^{-} + 0.5Pb^{+2}_{1/2}[O^{-}BO_{2/2}].$$

The presence of such BO_3 and BO_4, PbO_4 units in the $[(PbO)_{0.20-x}\cdot(Bi_2O_3)_{0.40}\cdot(B_2O_3)_{0.40}]$:$(TiO_2)_x$ glass network is evident from infrared spectra. Out of all these units, BO_4 units are expected to link to two other such units and one oxygen from each unit with a metal ion and thus the structure leads to the formation of long tetrahedron chains.

Bi_2O_3 is an incipient glass network former and as such does not readily form glass but does so in the presence of modifiers like PbO with triangular BiO_3 pyramids. The coordination of bismuth in the glass network can be viewed as tetrahedrons with the oxygen at three corners and $6s^2$ stereo chemically active electronic lone pair at the fourth corner.

Titanium ions are expected to exist mainly in Ti^{4+} state in the $[(PbO)_{0.20-x}\cdot(Bi_2O_3)_{0.40}\cdot(B_2O_3)_{0.40}]$:$(TiO_2)_x$

glass network, since in the starting batch, the starting chemical compound is TiO_2, in which the oxidation state of titanium ion is Ti^{4+}. However, reduction of Ti^{4+} to Ti^{3+} appears to be viable during melting quenching and subsequent annealing and crystallization processes of the glasses. Earlier reports on some other glass systems containing TiO_2 suggested that, upon heating at about 700 °C, there is a possibility for the reduction of Ti^{4+} ions to Ti^{3+} ions [40]. Further, the reduction, $Ti^{4+} + e = Ti^{3+}$, takes place only with $E_{\bigcirc} = 0.2$ V. The Ti^{4+} ions occupy both tetrahedral and substitutional octahedral and Ti^{3+} ions occupy modifying positions in six-fold coordination as corner-sharing $[TiO_6]^{2-}$ units in the glass network. TiO_4 and TiO_6 units of Ti^{4+} ions enter the glass network, alternate with BO_4 structural units and form linkages of the type B-O-Ti. In the IR spectra of $[(PbO)_{0.20-x}{\cdot}(Bi_2O_3)_{0.40}{\cdot}(B_2O_3)_{0.40}]{:}(TiO_2)_x$ glasses, with an increase of TiO_2 from 0.8 to 2.0 mol%, the band due to more ordered BO_4 structural units is observed to grow at the expense of the band due to BO_3 structural units; this observation indicates a gradual reduction in the degree of disorder in the glass network.

The band observed in the IR spectra between 640–650 cm^{-1} is due to Ti-O-Ti symmetric stretching vibrations of such TiO_6 units [33–38]. The TiO_6 octahedrons may be viewed as entwined with BO_4 structural units forming $TiBO_9$ where all the oxygens are bridging

Nevertheless, as has been mentioned earlier, these ions also present in the glass network with TiO_4 structural units; the band observed in the IR spectra between 730–740 cm^{-1} in fact represents vibrations due to such tetragonal units [32]. Tetragonally positioned Ti^{4+} ions do not induce any non-bridging oxygen ions but octahedrally positioned ions may do so [32] similar to Ti^{3+} ions. The highest intensity of the band due to TiO_4 structural units observed in the IR spectrum of the sample T_{20} indicates the presence of titanium ions largely in tetragonal positions or substitutional positions; in view of this, we may attribute the highest rigidity to this sample among all other glasses under investigation. When the concentration of TiO_2 is raised from 0 to 0.8 mol% in the glass network, the intensity of the band Ti-O vibrations of octahedral units is observed to increase, indicating a rise in the degree of disorder in the glass network when TiO_2 is present in this concentration range.

The electronic configuration of Ti^{3+} ion is $3d^1$ with ^2D ground state. In octahedral field or tetrahedral filed, the ^2D levels splits into ^2E and $^2T_2$ states. In the tetragonally distorted octahedral field the $^2T_2$ state further splits into three $^2B_2$ (i.e. $|xy\rangle$, $|yz\rangle$, and $|zx\rangle$) states, whereas the ^2E excited state splits into $A_1 \left|3z^2 - r^2\right\rangle$ and $B_1 \left|x^2 - y^2\right\rangle$ states by tetragonal distortion. The optical absorption and ESR spectra of Ti^{3+} ions is just similar to vanadyl complexes, where V^{4+} ions exists in octahedral coordination with tetrahedral compression [40]. For d^1 ions in tetragonally compressed octahedron, the ground state is $B_2 |xy\rangle$. Using Tanabe-Sugano diagrams for d^1 ions, the bands observed in the optical absorption spectra at about 530 nm and 690 nm are assigned respectively to $^2B_{2g} \rightarrow {}^2B_{1g}$ and $^2B_{2g} \rightarrow {}^2A_{1g}$ transitions of $3d^1$ electron of the Ti^{3+} ions. With increase in concentration of TiO_2 from 0.8 to 2.0 mol% in the sample, these bands are observed to shift towards lower wavelength with decreasing intensity. These observations indicate: i) a decrease in the concentration of Ti^{3+} ions and ii) stronger ligand field of existing Ti^{3+} ions.

The resonance signal observed in ESR spectra at g =1.94 is due to tetragonally compressed octahedral sites of Ti^{3+} ions with $|xy\rangle$ ground state [41]. The spectrum of each sample shows a triplet; such a triplet pattern of components may be ascribed to the hyperfine interaction of an unpaired electron with two equivalent $I = 1/2$ nuclear spins. Negative g shifts (g–go ~ -1.0) is attributable to small trigonal field splittings ($\delta^{¨} \sim$ 0.01 eV) of the low-lying orbital triplet resulting from the predominant octahedral field [42]. The relatively high intensity of these pattern observed in the spectrum of sample T_8 suggests a higher rate of reduction of Ti^{4+} ions to Ti^{3+} ions. As has been mentioned earlier, these Ti^{3+} ions, occupying modifying positions, create more dangling bonds; as a result there is an increase in the concentration of BO_3 structural units at the expense of BO_4 units (in the concentration range of 0 to 0.8 mol% of TiO_2). This is in accordance with the observations in the IR spectra.

Among various electric polarizations (electronic, ionic, dipolar and space charge polarizations) that contribute to the dielectric constant, the space charge polarization depends on the perfection of the glasses.

Recollecting the data, on the dielectric properties of $[(PbO)_{0.20-x}\cdot(Bi_2O_3)_{0.40}\cdot(B_2O_3)_{0.40}]:(TiO_2)_x$ glasses, a substantial hike in the values of the dielectric parameters (with respect to those of TiO_2-free glasses) is observed with increase in concentration of TiO_2 up to 0.8 mol%; such an increase is obviously due to the presence of larger concentration of titanium ions in Ti^{3+} state. These ions act as modifiers similar to any conventional modifier ions and generate bonding defects by breaking the bonds B-O-B, B-O-Ti, Bi-O-Pb, etc. The defects thus produced create easy pathways for the migration of charges that would build up space charge polarization and facilitate increase in the dielectric parameters as observed [43–45]. The decrease in the dielectric parameters with in the increase in the concentration of TiO_2 beyond 0.8 mol% in the glass matrix obviously suggests a decreasing disorder in the glass network.

The way the dielectric constant and the loss vary with the frequency and temperature suggests that these glasses exhibit dielectric relaxation effects. Conventionally, the dielectric relaxation effects are described with the variable frequency at a fixed temperature. However, similar information can also be obtained by analyzing these results at a fixed frequency at variable temperature as suggested by Bottcher and Bordewijk [46].

Substituting the equation (1) in standard Debye's relations for dielectric relaxation, one can obtain

$$\varepsilon'(\omega,T) = \varepsilon_\infty + \frac{1}{2}(\varepsilon_s - \varepsilon_\infty)\,[1 - tgh(E_a/RT + \ln \omega A)] \tag{4}$$

$$\varepsilon''(\omega,T) = \frac{\frac{1}{2}(\varepsilon_s - \varepsilon_\infty)}{\cosh(E_a/RT + \ln \omega A)}. \tag{5}$$

In equation (4) and (5) ε_∞ is temperature independent whereas ε_s is largely dependent on temperature. Keeping in mind the variation of hyperbolic trigonometric functions in equations (4) and (5) with temperature is very minute, these equations can be rewritten as

$$\varepsilon'(\omega,T) = \varepsilon_\infty + \frac{1}{2}(\varepsilon_s - \varepsilon_\infty)\,\{1 - tgh\,[E_a(1/T - 1/T_m(\omega))/R]\} \tag{6}$$

and

$$\varepsilon''(\omega,T) = \frac{\frac{1}{2}(\varepsilon_s - \varepsilon_\infty)}{\cosh\,[E_a(1/T - 1/T_m(\omega))/R]}. \tag{7}$$

In these equations $T_m(\omega)$ is the peak temperature at where ε' exhibits maximum value. Thus as per equations (4) and (5), the plots of $\varepsilon'(\omega,T)$ and $\varepsilon''(\omega,T)$ against $1/T$ should be centro-symmetric and symmetric curves respectively in the dielectric relaxation region. As an example, for one of the glasses (viz., T_8) under investigation, the variation of $\varepsilon'(\omega,T)$ and $\varepsilon''(\omega,T)$ with $1/T$ are shown in Figure 10. The shape of these curves is well in accordance with the equations (4) and (5) and clearly confirms the relaxation character of dielectric properties of these glasses.

Further, to know whether there is single relaxation time or spreading of relaxation times for the dipoles, we have adopted a pseudo Cole-Cole plot method (instead of the conventional Cole-Cole plot) between $\varepsilon'(\omega)$ and $\varepsilon''(\omega)$ at a fixed temperature) suggested by Sixou [47], in which $\varepsilon'(T)$ versus $\varepsilon''(T)$ can be plotted at a fixed frequency. The nature of variation of $\varepsilon'(T)$ and tan δ with temperature for these glasses indicates that the Cole-Davidson equation

$$\varepsilon^*(\omega) = \varepsilon_\infty + \frac{\varepsilon_s - \varepsilon_\infty}{(1 + i\omega\tau)^\beta} \tag{8}$$

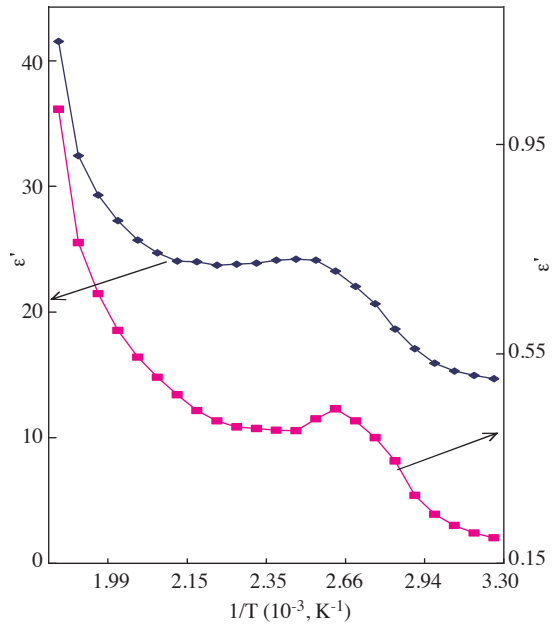

Figure 10. Variation of $\varepsilon'\omega$ (T) and ε'' (ω,T) with $1/T$ for glassT_8.

can safely be applied to these glasses. Separating real and imaginary terms of equation (6), and rewriting with explicit temperature dependence of terms:

$$\varepsilon'(\omega,T) = \varepsilon_\infty + (\varepsilon_s - \varepsilon_\infty)[\cos\varphi(T)]^\beta \cos\beta\varphi(T) \tag{9}$$

and

$$\varepsilon''(\omega,T) = (\varepsilon_s - \varepsilon_\infty)[\cos\varphi(T)]^\beta \sin\beta\varphi(T), \tag{10}$$

where

$$\varphi(T) = \tan^{-1}(\omega\tau) = \tan^{-1}(\omega A_o e^{W_d/KT}). \tag{11}$$

In equation (11) A_o is a constant and W_d is the activation energy for the dipoles. The plot between $\varepsilon'(T)$ and $\varepsilon''(T)$, given by equations (9) and (10) at a fixed frequency, is often called a pseudo Cole-Cole plot, which cuts ε' axis at ε_s and ε_∞ Here, ε_s is known as high temperature dielectric constant and ε_∞ is the low temperature dielectric constant. The plot cuts ε' axis (as per Sixou) at low temperature side at an angle of $(\pi/2)\beta$ here β is the spreading factor for relaxation times. For the glass containing 0.6% of TiO_2 (glass T_6), a pseudo Cole-Cole plot at 10 kHz is shown in Figure 11. The spreading factor β estimated from this plot is 0.68 radians; such plots have also been drawn for all the glasses and the value of β is estimated in a similar way; the value of β is found to increase gradually when concentration of TiO_2 is raised in the glass matrix up to 0.8 mol% (see Table 2). Earlier studies on the glasses containing d^1 ions such as W^{5+}, Cr^{5+}, Ti^{3+}, Mo^{5+}, etc., showed that these ions contribute to the dielectric relaxation effects [18, 29, 48–50]. Hence, based on these reports, the dipolar effects exhibited by TiO_2 mixed glasses can safely be attributed to Ti^{3+} ions. The spreading of relaxation times in these glasses may be understood due to the dipoles experience an approximately random potential energy on diffusing through the distorted structure $[(PbO)_{0.20-x}{\cdot}(Bi_2O_3)_{0.40}{\cdot}(B_2O_3)_{0.40}]{:}(TiO_2)_x$ glass network [51]. The shifting of relaxation region towards lower temperatures and decrease in the activation energy for the dipoles with increase in the concentration of TiO_2 from 0 to 0.8 mol% (Table 3) suggests an increasing degree of freedom for dipoles to orient in the field direction in the glass network. The increase in the intensity of the relaxation effects up to 0.8 mol% of TiO_2 further supports the earlier argument that, there is an increasing reduction of Ti^{4+} ions into Ti^{3+} state that take modifying positions.

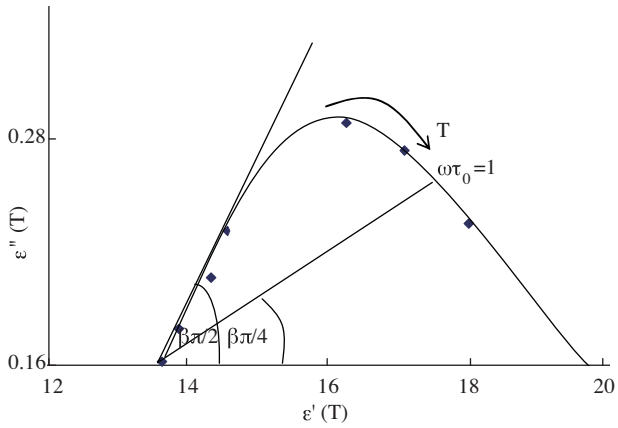

Figure 11. A pseudo Cole-Cole plot drawn at 10 kHz for the glass T_6.

When a plot is made between log $\sigma(\omega)$ *vs.* activation energy for conduction (in the high temperature region) a near linear relationship is observed (see Figure 12); this observation suggests that the conductivity enhancement is directly related to the thermally stimulated mobility of the charge carriers in the high temperature region. The conductivity isotherm as a function of the concentration of TiO_2 passes through a maximum at $x = 0.8$ mol% (see inset 'b' in Figure 5). The figure obviously suggests a kind of transition from predominantly ionic to electronic conductivity [52, 53]. With the entry of highly mobile conducting ions in to the glass network, the electronic paths are progressively blocked causing an inhibition of the electronic current with a simultaneous increase in the ionic transport. The mobile electrons, or polarons, involved in the process of transfer from $Ti^{3+}$to Ti^{4+} are attracted by the oppositely charged cations. This cation-polaron pair moves together as a neutral entity. As expected, the migration of this pair is not associated with any net displacement of the charge and thus does not contribute to electrical conductivity, as a result, a decrease in the conductivity results beyond 0.8 mol% of TiO_2.

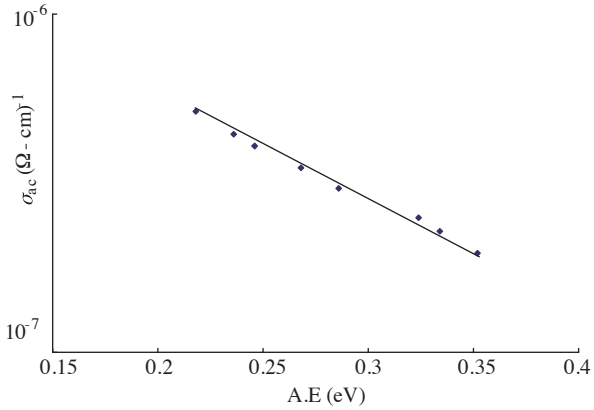

Figure 12. Variation of activation energy with the a.c. conductivity.

Our observations on dielectric parameters of $[(PbO)_{0.20-x}{\cdot}(Bi_2O_3)_{0.40}{\cdot}(B_2O_3)_{0.40}]{:}(TiO_2)_x$ glasses, as mentioned earlier, indicate the rate of increase of $\varepsilon' \tan\delta$ (which is inversely proportional to break down strength) with temperature is the highest for glass T_8 and the lowest for the glass T_{20}. Thus the experiments on dielectric properties of these glasses also reveal that there is an increase in the dielectric breakdown strength of the glasses with increase in the concentration of TiO_2 beyond 0.8 mol%. These revelations are also consistent with the view that in the concentration range of 0.8 to 2.0 mol%, the titanium ions mostly exist in Ti^{4+} state and occupy network forming positions with TiO_4 structural units and increase the rigidity of the glass network.

5. Conclusions

The summary of the data from the study of various physical properties of $[(PbO)_{0.20-x}\cdot(Bi_2O_3)_{0.40}\cdot(B_2O_3)_{0.40}]$:$(TiO_2)_x$ glasses is as follows:

1. Optical absorption studies indicate that the presence of titanium ions predominantly in Ti^{3+} state when the concentration of TiO_2 is in the range 0.2–0.8 mol%.
2. The analysis of ESR spectra and the magnetic susceptibility data indicated that in the sample T_8, maximum reduction of titanium ions from Ti^{4+} to Ti^{3+}.
3. IR spectral studies point out a gradual increase in the degree of disorder of the glass network with increase in the concentration of TiO_2 up to 0.8 mol%, beyond which there is decrease in the disorder of the glass network.
4. The dielectric parameters $\varepsilon\prime$, tan δ and σ_{AC} are found to increase and the activation energy for AC conduction is found to decrease with a increase in the concentration of TiO_2 up to 0.8 mol%, indicating an increase in the concentration of titanium ions that take part modifying positions in this concentration range.
5. Variation of tan δ with temperature exhibited dipolar relaxation effects; the effects were analyzed with pseudo Cole-Cole plots spreading of relaxations with the set of relaxation times τ has been established.
6. The a.c conduction in the high-temperature region seems to be connected with both electronic and ionic. More specifically, up to 0.8 mol% of TiO_2 the ionic conduction seems to be dominant while in the higher concentration range, the electronic conduction seems to prevail.

In conclusion with in the concentration range of 0.2 to 0.8 mol%, titanium ions predominantly exist in Ti^{3+} state, and from 1.0 to 2.0 mol% these ions seem to be mainly in Ti^{4+} state.

References

[1] K. Nassau and D. L. Chadwick, *J. Am. Ceram. Soc.,* **65**, (1982), 486.

[2] R. Luciana, P. Kassab, H. Sonia Tatumi, C. M. S. Mendes, C. Lilia. Courrol, Niklaus and U. Wetter, *Optics Express,* **6**, (2000), 104.

[3] L. Baia, R. Stefan, W. Kiefer, J. Popp and S. Simon, *J. Non-Cryst. Solids*, **303**, (2002), 379.

[4] D. K. Durga and N. Veeraiah, *J. Mater. Sci.*, **36**, (2001), 5625.

[5] C. H. Kim, H. L. Park and S. Mho, *Solid State Commun.*, **101**, (1997), 109.

[6] A. M. Strivastava, *J. Lumin.*, **78**, (1998), 239.

[7] I. V. Kityk, J. Wasylak, D. Dorosh, J. Kucharski and A. Brenier, *Mater. Lett.*, **49**, (2001), 272; I. V. Kityk, E. Golis, J. Filipecki, J. Wasylak and V. M. Zacharko, *J. Mater. Sci. Lett.*, **14**, (1995), 1292.

[8] S. R. Lacerda, J. M. Oliveria, R. N. Correia, M. H. V. Fernandes, *J. Non-Cryst. Solids*, **221**, (1997), 235.

[9] L. Koudelka, P. Mosner, M. Zeyer and C. Jager, *J. Non-Cryst. Solids*, **326**, (2003), 72.

[10] N. Shimoji, T. Hashimoto, H. Nasu and K. Kamiya, *J. Non-Cryst. Solids*, **324,** (2003), 50.

[11] A. Shaim and M. Et–tabirou, *J. Mater. Chem. Phys.*, **80,** (2003), 63.

[12] R. Balaji Rao, D. Krishna Rao and N. Veeraiah, *Mater.Chem.Phys.*, **87**, (2004), 357.

[13] R. K. Brow, W.L. Warren, A. McIntyre and D. E. Day, *Phys. Chem. Glasses*, **38**, (1997), 300.

[14] E. Lines, *Phys. Rev. B,* **43**, (1991), 11978.

[15] M. Sheik-Bahae, D. J. Hagan and E. Van Stryl, *J. Quantum electron*, **27**, (1991), 296.

[16] Y. Watanabe, M. Ohnishi and T. Tsuchiya, *Appl. Phys. Lett.*, **66,** (1995), 3431.

[17] K. Sambasiva Rao, M. Srinivasa Reddy and N. Veeraiah, *Physica B*, **396**, (2007), 29; M. Srinivasa Reddy, S.V.G.V.A. Prasad, and N. Veeraiah, *Phys. Status Solidi (a)*, **204,** (2007), 816.

[18] G. Murali Krishna, B. Anila Kumari, M. Srinivasa Reddy and N. Veeraiah, *J. Solid State Chem.* DOI:10.1016/j.jssc.2007.07.025

[19] M. H. Kin, Y. H. Jeong, S. Nahm, H. T. Kim and H. J. Lee, *J. Euro. Ceram. Soci.,* **26**, (2006), 2139

[20] P. Bergo, W. M. Pontuschka and J. M. Prison, *Mater. Chem. Phys.*, **108**, (2008), 142.

[21] Y. Sereda, I. Y Polishchuk and A. L. Burin, *Phys. Rev. B,* **75**, (2007), 024207.

[22] S.V.G.V.A. Prasad, M. Srinivasa Reddy and N. Veeraiah, J. *Phys. Chem. Solids,* **67**, (2006), 2478.

[23] N. Krishna Mohan, K. Sambasiva Rao, Y. Gandhi and N. Veeraiah, *Physica B,* **387**, (2007), 213.

[24] X. Zhu, Q. Li, N. Ming and Z. Meng, *Appl. Phys. Lett.*, **71,** (1997), 867.

[25] A. A. Boukais, D. Bogomolova, A. A. Deshkovskaya, V. A. Jachkin, S. A. Prushinsky, N. A. Krssil Nikova, O. A. Trul, S. V. Stefanovsky and E. A. Zhilinskaya, *Optical Mater.*, **19**, (2002), 295.

[26] B. V. Raghavaiah, C. Laxmikanth and N. Veeraiah, *Optics Commun.*, **235**, (2004), 341.

[27] F. A. Khalifa, H. A. El Batal and A. Azooz, *Ind. J. Pure & Appl. Phys.*, **36**, (1998), 314.

[28] K. J. Rao, *Structural Chemistry of Glasses*, Elsevier, Amsterdam, 2002.

[29] G. Srinivasarao and N. Veeraiah, *J. Solid State Chem.*, **166**, (2002),104.

[30] N. Krishna Mohan, G. Sahaya Bhaskaran and N. Veeraiah, *Phys stat solidi (a)*, **203**, (2006), 2083.

[31] S. Hazra and A. Ghosh, *The American Physical Soc.*, **51**, (1995), 851.

[32] M. Belkhouaja, M. Et-Tabirou and M. Elmoudane, *Phase Transitions*, **76**, (2003), 645.

[33] T. Kokubo and Y. Inaka, *J. Non-Cryst. Solids,* **95**, (1987), 547.

[34] K. H. Jo and K. H. Yoon, *Mat. Res. Bull.,* **24**, (1989), 1.

[35] Y. Dimitriev, V. Mihailova, V. Dimitrov and Y. Ivanova, *J. Mater. Sci. Lett.*, **10**, (1991), 1249.

[36] A. Shaim and M. Et-Tabirou, *J. Mater. Chem. Phys.*, **80**, (2003), 63.

[37] A. Shaim, M. Et-Tabirou, L. Montagne and G. Palavit, *Mater. Res. Bull.*, **37**, (2002), 2459.

[38] G. Laudisio, M. Catauro, A. Aronne and P. Pernice, *Thermo-Chem. Acta*, **94**, (1997), 173.

[39] P. J. Bray, M. Leventhal and H. O. Hooper, *Phys. Chem. Glasses.*, **4,** (1963), 47

[40] B. V. R. Chowdari, G. V. Subba Rao, G. Y. H. Lee and X. P. Sand, *Solid state ionics,* **136**, (2000), 1067.

[41] I. Abrahams and E. Hadzifejzovic, *Solid State Ionics*, **134**, (2000), 249.

[42] D. L. Griscom, *J. Non-Cryst. Solids*, **40**, (1980), 211.

[43] M. Srinivasa Reddy, V. L. N. Sridhar Raja and N. Veeraiah, *Eur. Phys. J. Appl. Phys.,* **37,** (2007), 203.

[44] S. G. Kim, H. Shin, J. S. Park, K. S. Hung, H. Kim, *J. Electroceramics*, **15**, (2005), 129.

[45] N. Krishna Mohan, G. Sahaya Baskaran and N. Veeraiah, *Phys. stat. sol. (a),* **203,** (2006), 2083.

[46] C. J. F. Bottcher and P. Bordewijk, *Thoery of electric polarization,* (Elsevier Scientific Publishing Company, Oxford 1978).

[47] P. Sixou, P. Dansas and D. Gillot, *J. Chem. Phys.*, **64**, (1967), 834.

[48] P. Subbalakshmi and N. Veeraiah, *J. Non-Cryst. Solids*, **298**, (2002), 89.

[49] G. Murali Krishna, N. Veeraiah, N. Venkatramaiah and R. Venkatesan, *J Alloys and Comp.*, **450,** (2008), 477.

[50] R. M. Abdelouhab, R. Braunstein and K. Baerner, *J. Non-Cryst. Solids,* **108**, (1989), 109.

[51] S. R. Elliott, *Physics of Amorphous Materials*, (Longman, Essex 1999).

[52] R. A. Montani and M. A. Frechero, *Solid State Ionics,* **158,** (2003), 327.

[53] K. Sambasiva Rao, M. Srinivasa Reddy and N. Veeraiah, *Physica B*, **396**, (2007), 29.